

Discriminate sensing of pyrophosphate using a new tripodal tetramine-based dinuclear Zn(II) complex under indicator displacement assay approach

Sarayut Watchasit,[†] Pattira Suktanarak,[‡] Chomchai Suksai,^{‡*} Vithaya Ruangpornvisuti[†] and Thawatchai Tuntulani ^{†*}

[†]*Department of Chemistry, Faculty of Science, Chulalongkorn University, Bangkok, Thailand, 10330.*

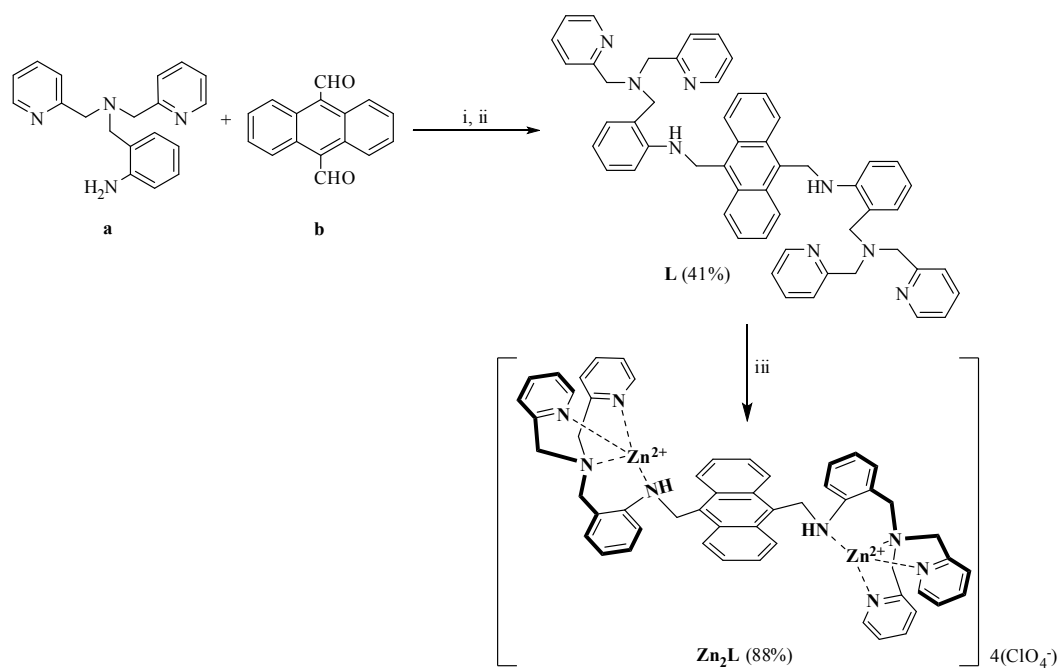
[‡]*Department of Chemistry and Center of Excellence for Innovation in Chemistry, Faculty of Science, Burapha University, Chonburi, Thailand, 20131.*

Content

Scheme S1	Synthetic procedure of ligand L and Zn₂L .	S3
Figure S1	¹ H-NMR spectrum of ligand L in CDCl ₃ .	S3
Figure S2	¹³ C-NMR Spectrum of ligand L in CDCl ₃ .	S4
Figure S3	¹ H-NMR spectrum of Zn₂L in 20% (v/v) D ₂ O/CD ₃ CN.	S4
Figure S4	¹³ C-NMR spectrum of Zn₂L in 20% (v/v) D ₂ O/CD ₃ CN.	S5
Figure S5	HMQC-NMR spectrum of Zn₂L in CD ₃ CN.	S5
Table S1	Total and relative energies of all the B3LYP/LANL2DZ-optimized structures of six conformers of the dimeric 2:2 species.	S6
Figure S6	DFT/B3LYP/LANL2DZ-optimized structure of the dimeric 2:2 species of C1 conformer.	S7
Figure S7	DFT/B3LYP/LANL2DZ-optimized structure of the dimeric 2:2 species of C2 conformer.	S8
Figure S8	DFT/B3LYP/LANL2DZ-optimized structure of the dimeric 2:2 species of C3 conformer.	S9
Figure S9	DFT/B3LYP/LANL2DZ-optimized structure of the dimeric 2:2 species of P1 conformer.	S10
Figure S10	DFT/B3LYP/LANL2DZ-optimized structure of the dimeric 2:2 species of P2 conformer.	S11
Figure S11	DFT/B3LYP/LANL2DZ-optimized structure of the dimeric 2:2 species of P3 conformer.	S12
Figure S12	¹ H NMR spectra of 1:1 ratio of ensemble formation between Zn₂L :MTB (5 mM) upon addition of various concentration of PPi	S13

(0.05 M) in 20% (v/v) D₂O:CD₃CN.

Figure S13	¹ H NMR spectra of 1:2 ratio of ensemble formation between Zn₂L:2MTB (5 mM) upon addition of various concentration of PPi (0.05 M) in 20% (v/v) D ₂ O:CD ₃ CN.	S14
Figure S14	³¹ P NMR spectra of [Zn₂L·MTB] (5 mM) upon addition of various concentration of PPi (0.05 M) in 20% (v/v) D ₂ O:CD ₃ CN.	S15
Figure S15	³¹ P NMR spectra of [Zn₂L·2MTB] (5 mM) upon addition of various concentration of PPi (0.05 M) in 20% (v/v) D ₂ O:CD ₃ CN.	S16
Figure S16	(a) UV/vis spectra obtained by addition of Zn₂L (400 μM) to a solution of indicator PV (20 μM) in HEPES buffered pH 7.4 in 20% (v/v) H ₂ O/CH ₃ CN solution, (b) Job's plot analysis of PV-Zn₂L ensemble. (c) A plot of absorption against concentration of Zn₂L titrated in PV Zn₂L ensemble	S17
Figure S17	(a) UV/vis spectra obtained by addition of Zn₂L (400 μM) to a solution of indicator BPG (20 μM) in HEPES buffered pH 7.4 in 20% (v/v) H ₂ O/CH ₃ CN solution, (b) Job's plot analysis of BPG-Zn₂L ensemble, C) A plot of absorption against concentration of Zn₂L titrated in BPG .	S18
Figure S18	(a) UV/vis spectra obtained by addition of Zn₂L (400 μM) to a solution of indicator XO (20 μM) in HEPES buffered pH 7.4 in 20% (v/v) H ₂ O/CH ₃ CN solution, (b) Job's plot analysis of XO-Zn₂L ensemble, C) A plot of absorption against concentration of Zn₂L titrated in XO .	S19
Figure S19	A plot of absorption against concentration of Zn₂L titrated in MTB .	S19
Figure S20	Calibration curve for detection of PPi using MTB-Zn₂L ensemble.	S20



Scheme S1. Synthetic procedure of **L** and **Zn₂L**. (i) acetonitrile, reflux 12 h, (ii) NaBH₄, MeOH, reflux 12 h, (iii) Zn(ClO₄)₂, EtOH, reflux 12 h.

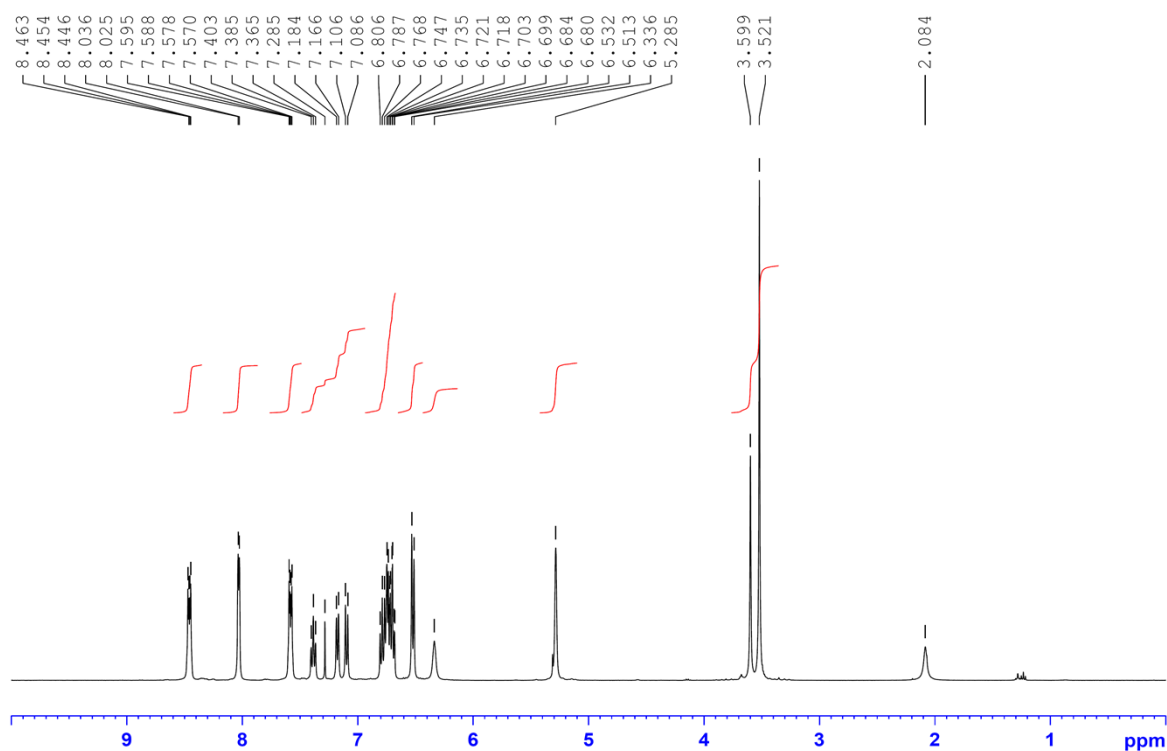


Figure S1. ¹H-NMR spectrum of ligand **L** in CDCl₃.

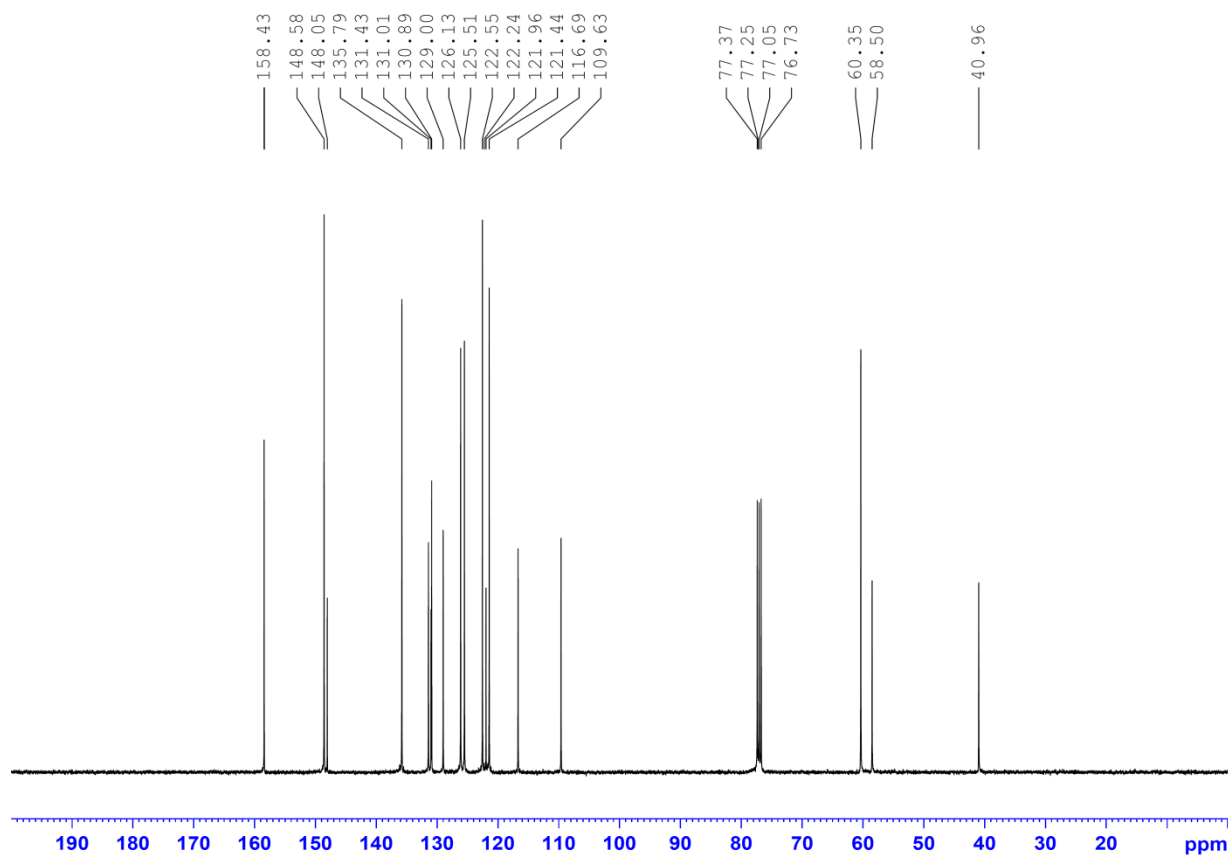


Figure S2. ^{13}C -NMR Spectrum of ligand **L** in CDCl_3 .

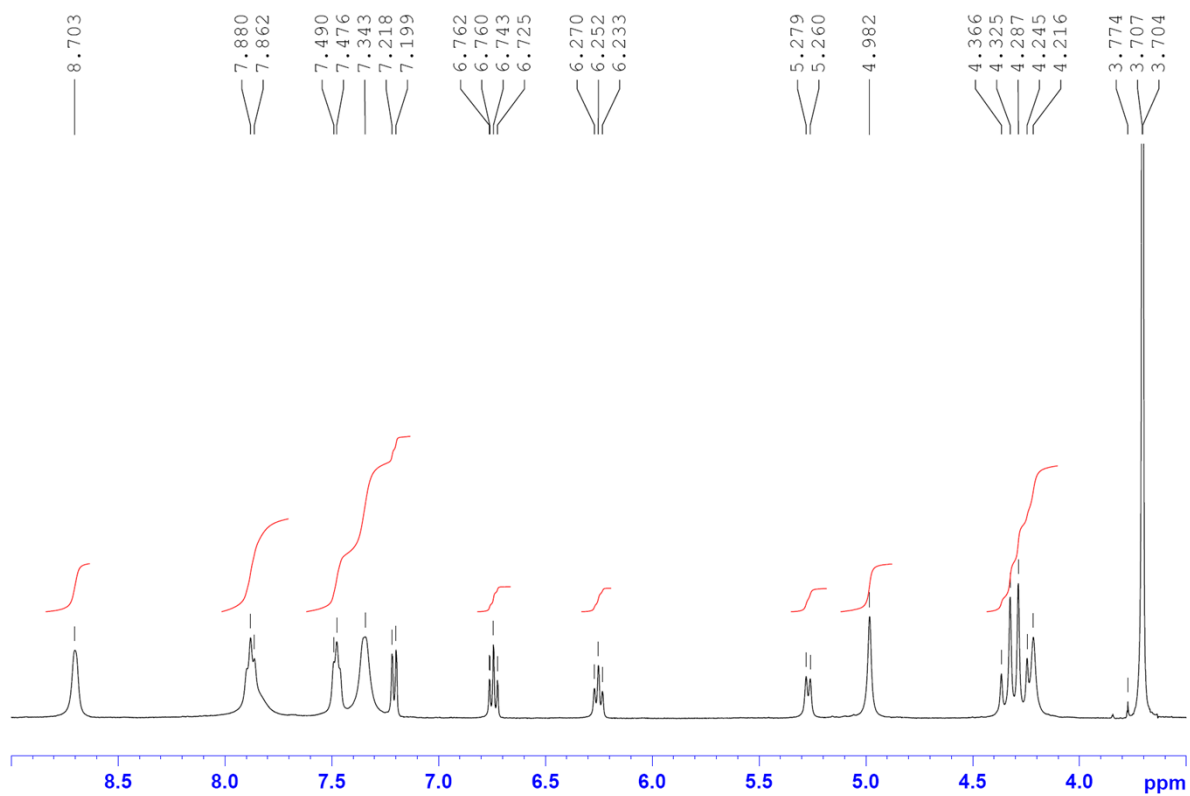


Figure S3. ^1H -NMR spectrum of Zn_2L in 20% (v/v) $\text{D}_2\text{O}/\text{CD}_3\text{CN}$.

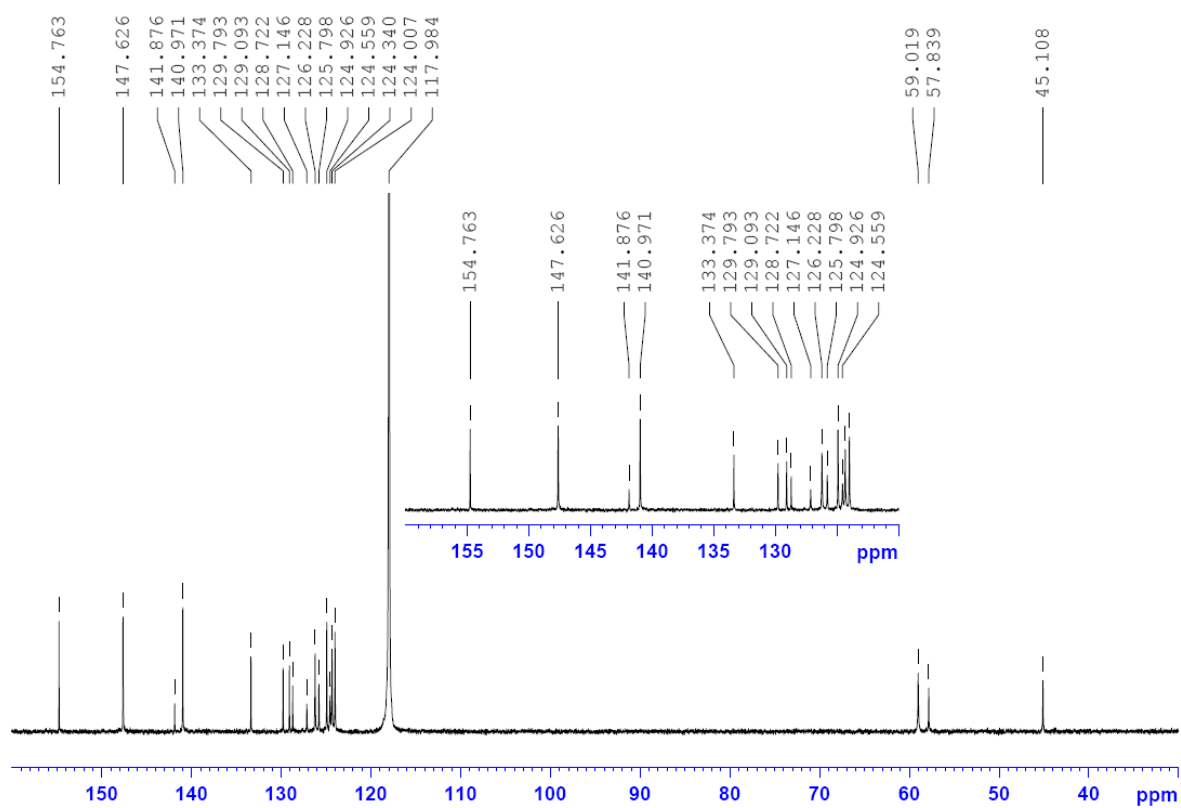


Figure S4. ¹³C-NMR spectrum of **Zn₂L** in 20% (v/v) D₂O/CD₃CN.

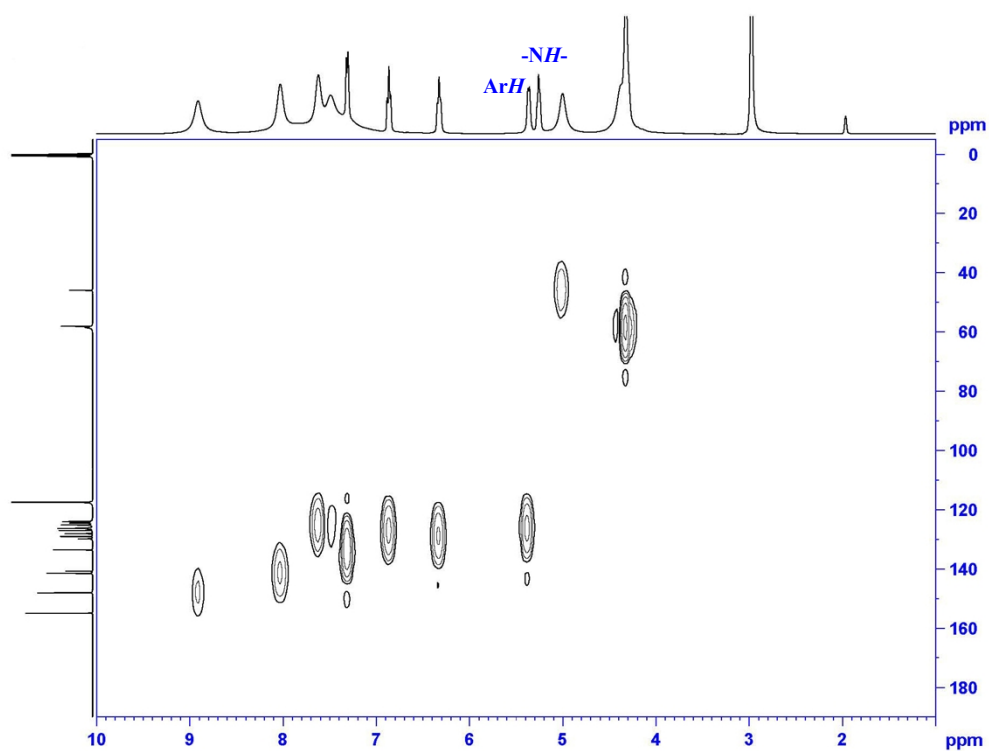


Figure S5. HMQC-NMR spectrum of **Zn₂L** in CD₃CN.

Table S1 Total and relative energies of all the B3LYP/LANL2DZ–optimized structures of six conformers of the dimeric 2:2 species.

Conformers ^a	E_{total} ^b	ΔE_{rel} ^c
C1	-6392.7827862	75.37
C2 ^d	-6392.9028947	0.00
C3	-6392.8176487	53.49
P1	-6392.7687205	84.20
P2	-6392.7596734	89.87
P3	-6392.7567471	91.71

^a Conformers are named according to cross (C) or parallel (P) alignment of two anthracene units of the dimeric species. ^b Total energies are in au. ^c Relative energies compared with the most stable conformer (C2), in kcal/mol. ^d The most stable conformer.

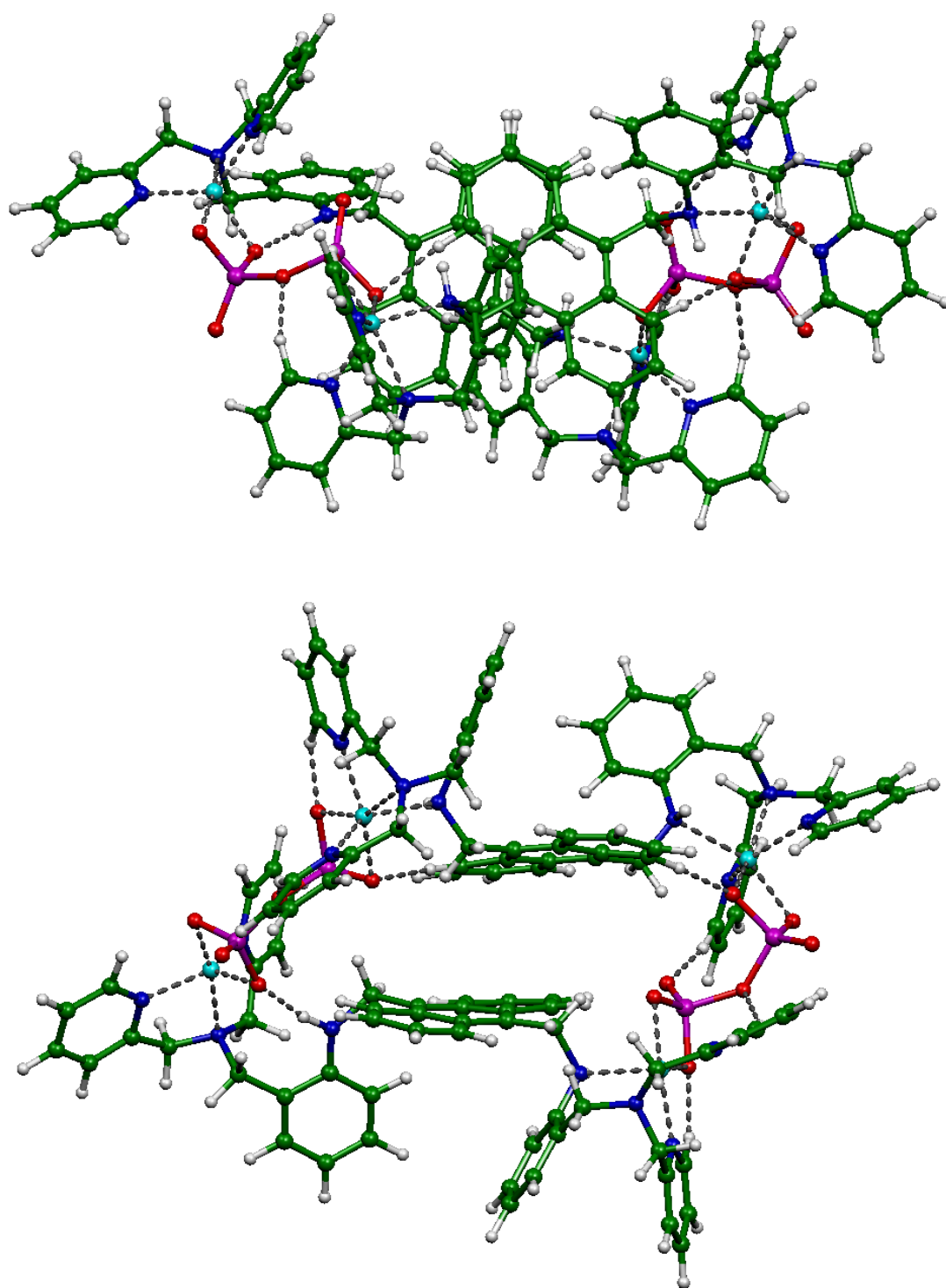


Figure S6. DFT/B3LYP/LANL2DZ-optimized structure of the dimeric 2:2 species of C1 conformer. Top and bottom images are top and front views, respectively.

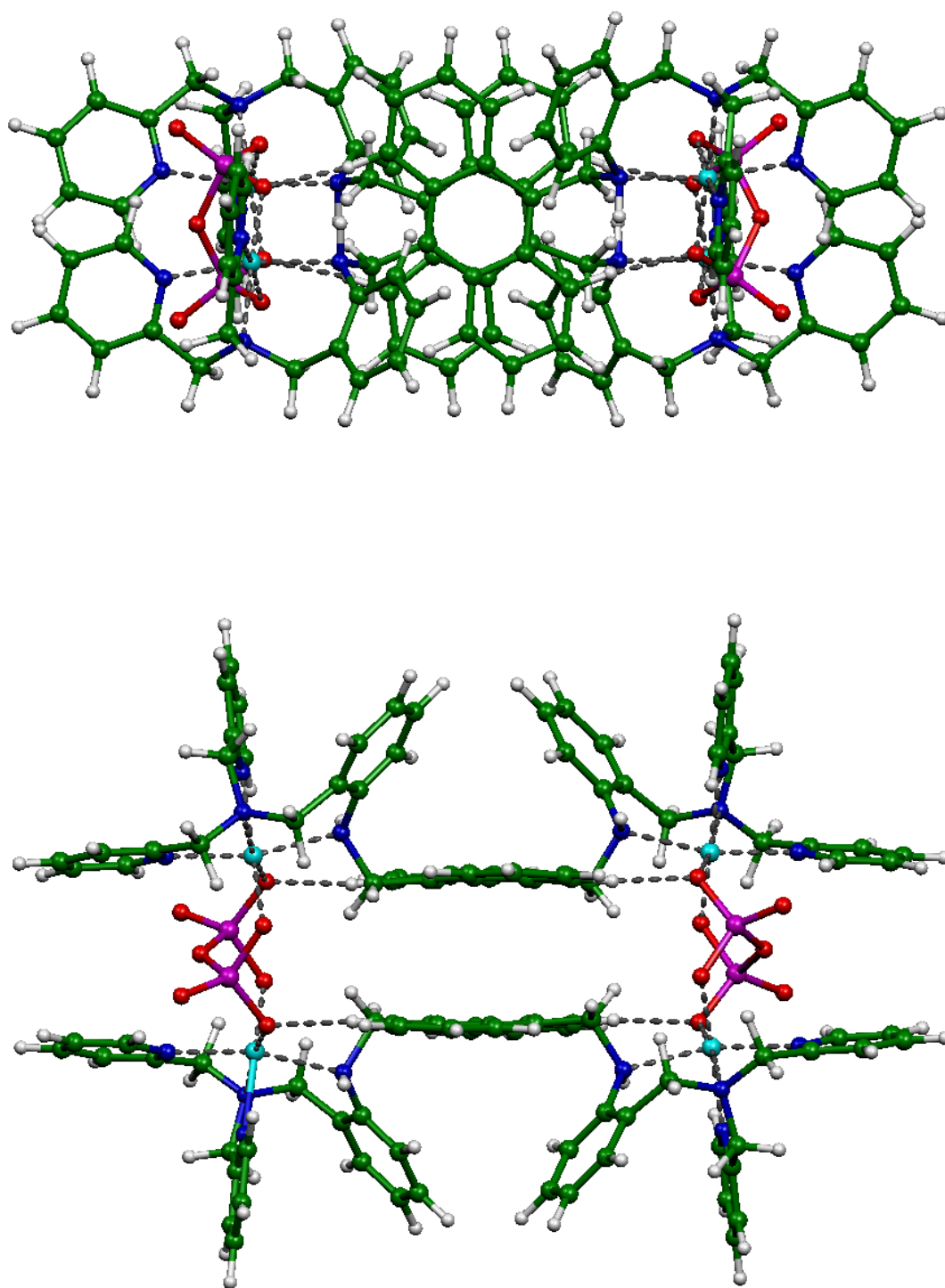


Figure S7. DFT/B3LYP/LANL2DZ-optimized structure of the dimeric 2:2 species of C2 conformer as the most stable one. Top and bottom images are top and front views, respectively.

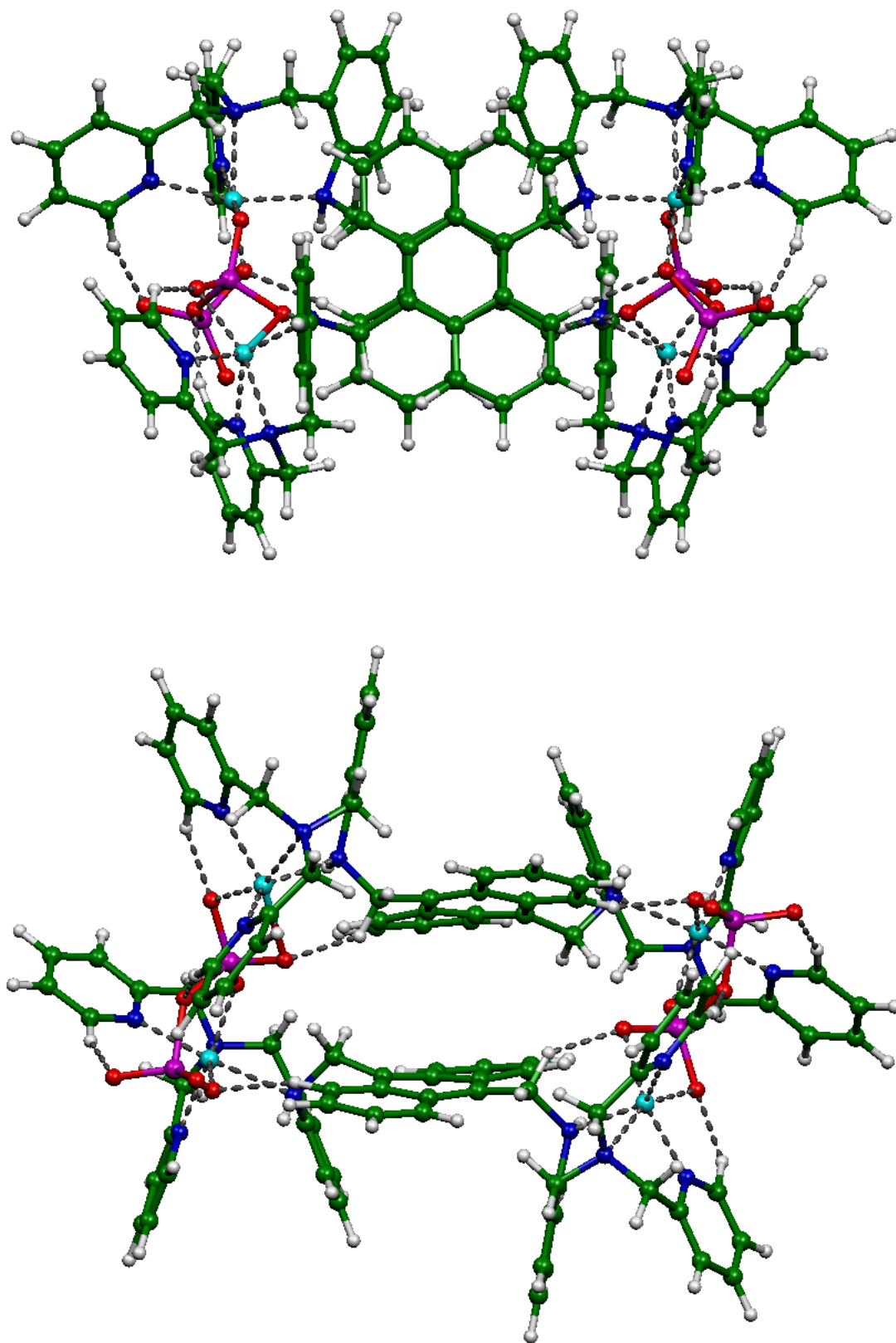


Figure S8. DFT/B3LYP/LANL2DZ-optimized structure of the dimeric 2:2 species of C3 conformer. Top and bottom images are top and front views, respectively.

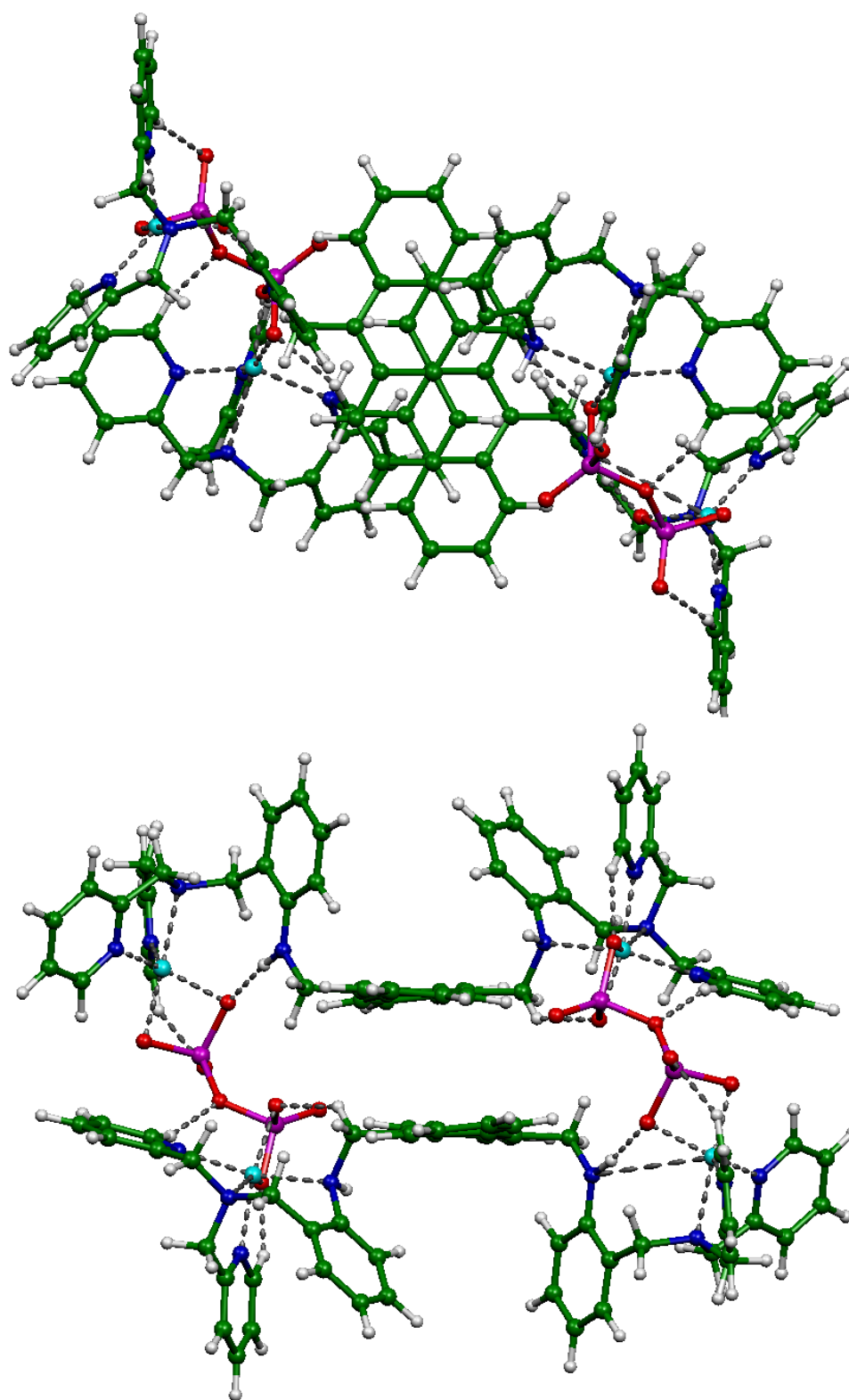


Figure S9. DFT/B3LYP/LANL2DZ-optimized structure of the dimeric 2:2 species of P1 conformer. Top and bottom images are top and front views, respectively.

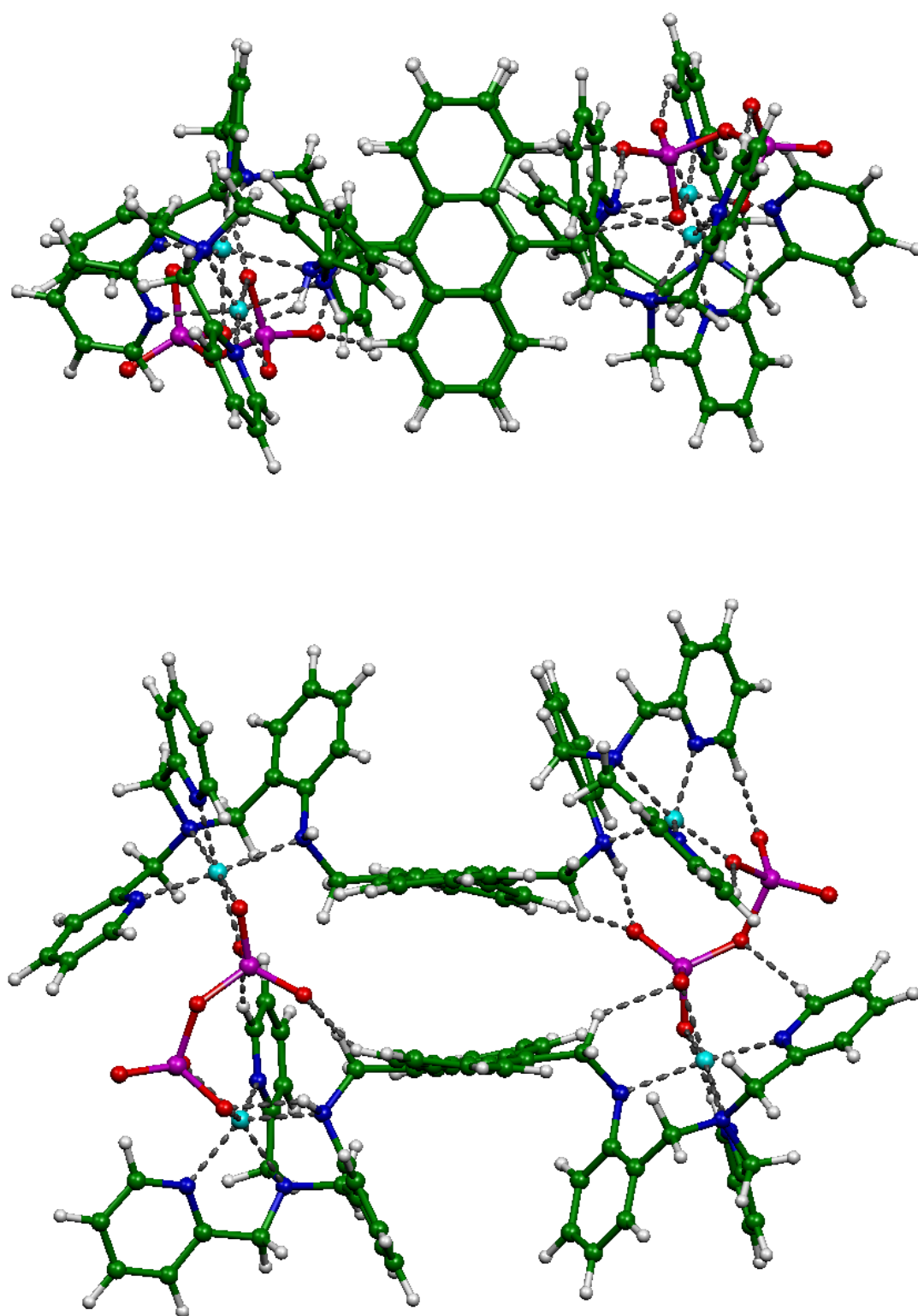


Figure S10. DFT/B3LYP/LANL2DZ-optimized structure of the dimeric 2:2 species of P2 conformer. Top and bottom images are top and front views, respectively.

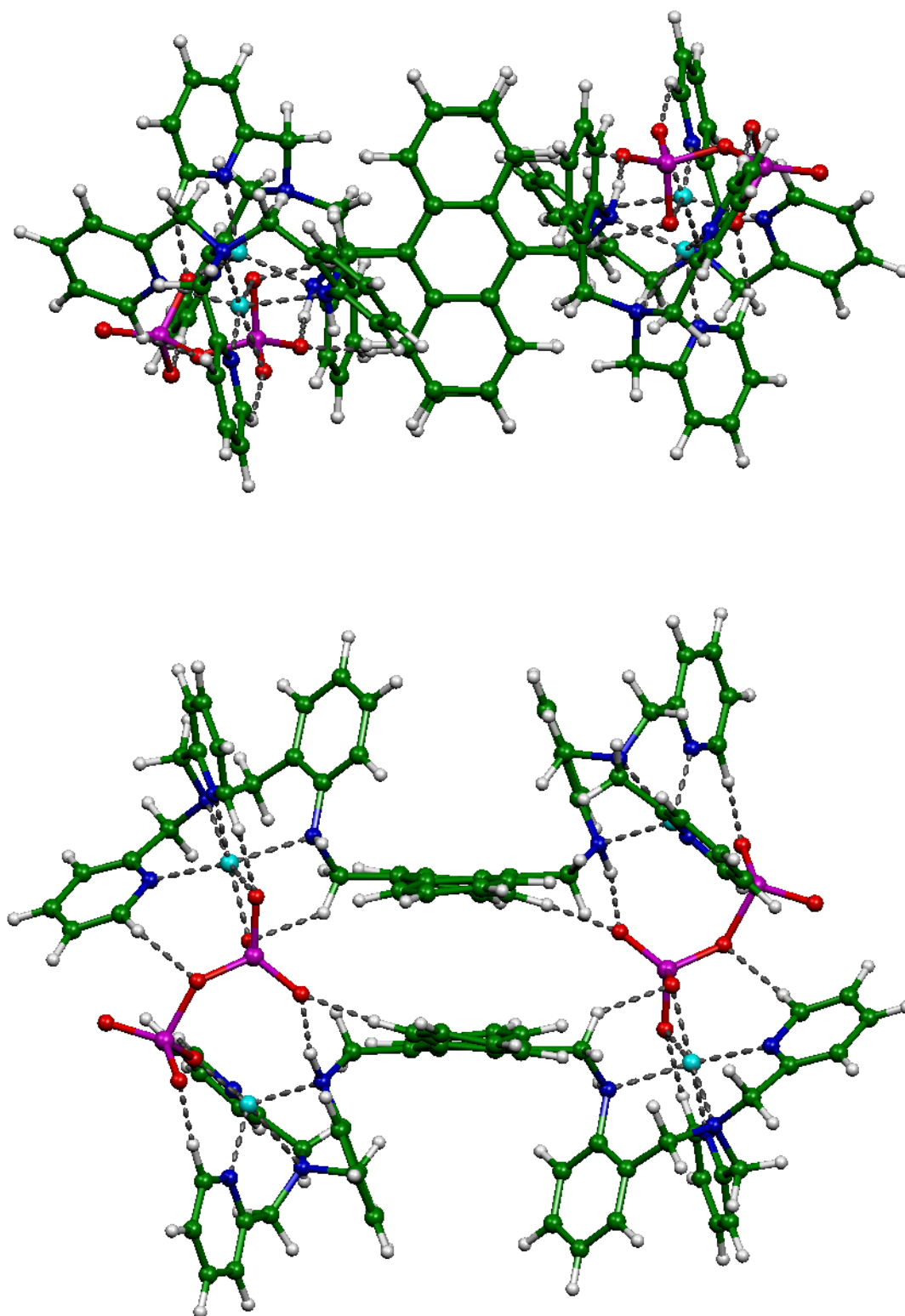


Figure S11. DFT/B3LYP/LANL2DZ-optimized structure of the dimeric 2:2 species of P3 conformer. Top and bottom images are top and front views, respectively.

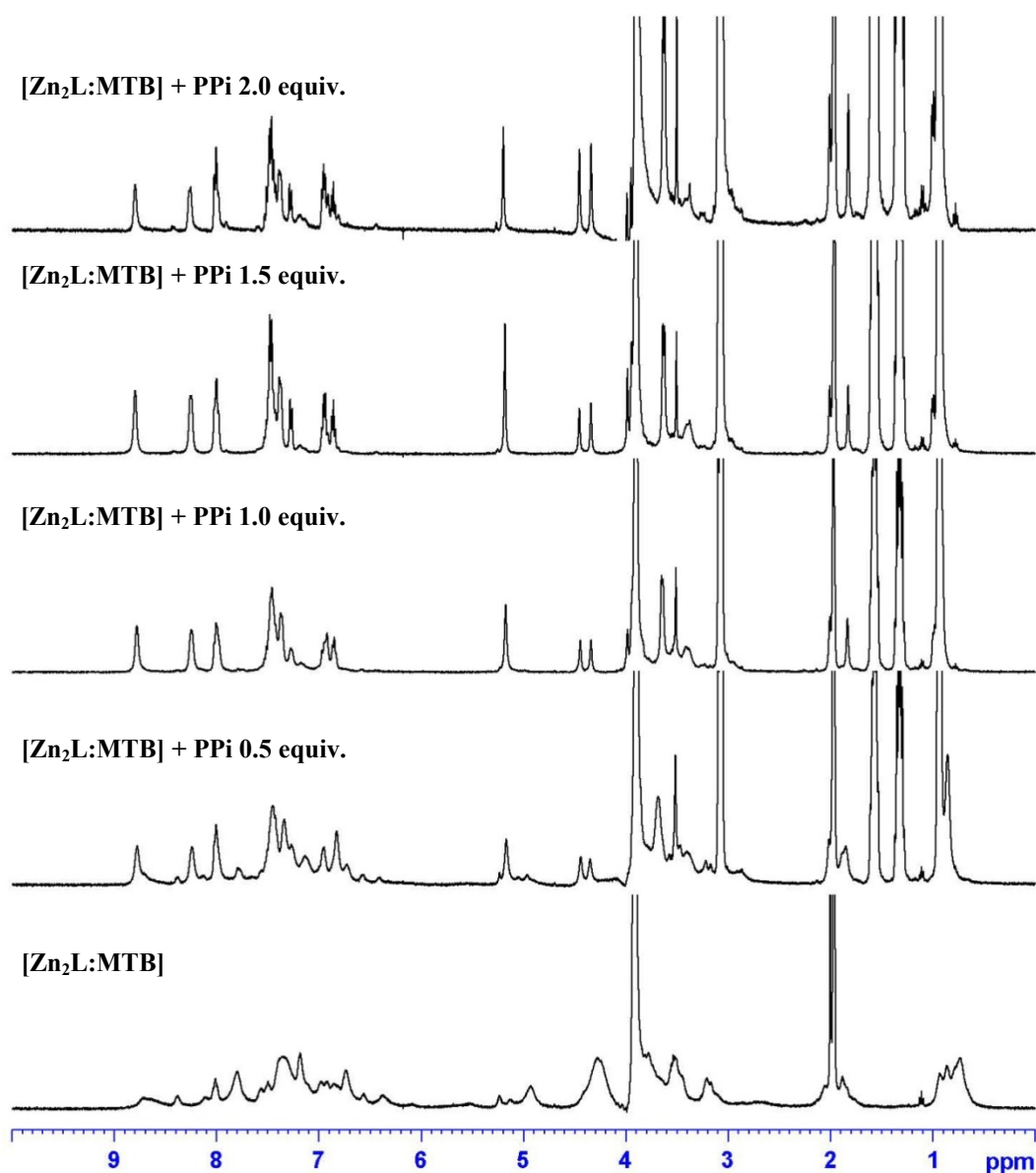


Figure S12. ^1H NMR spectra of 1:1 ratio of ensemble formation between $\text{Zn}_2\text{L:MTB}$ (5 mM) upon addition of various concentrations of **PPI** (0.05 M) in 20% (v/v) $\text{D}_2\text{O}:\text{CD}_3\text{CN}$.

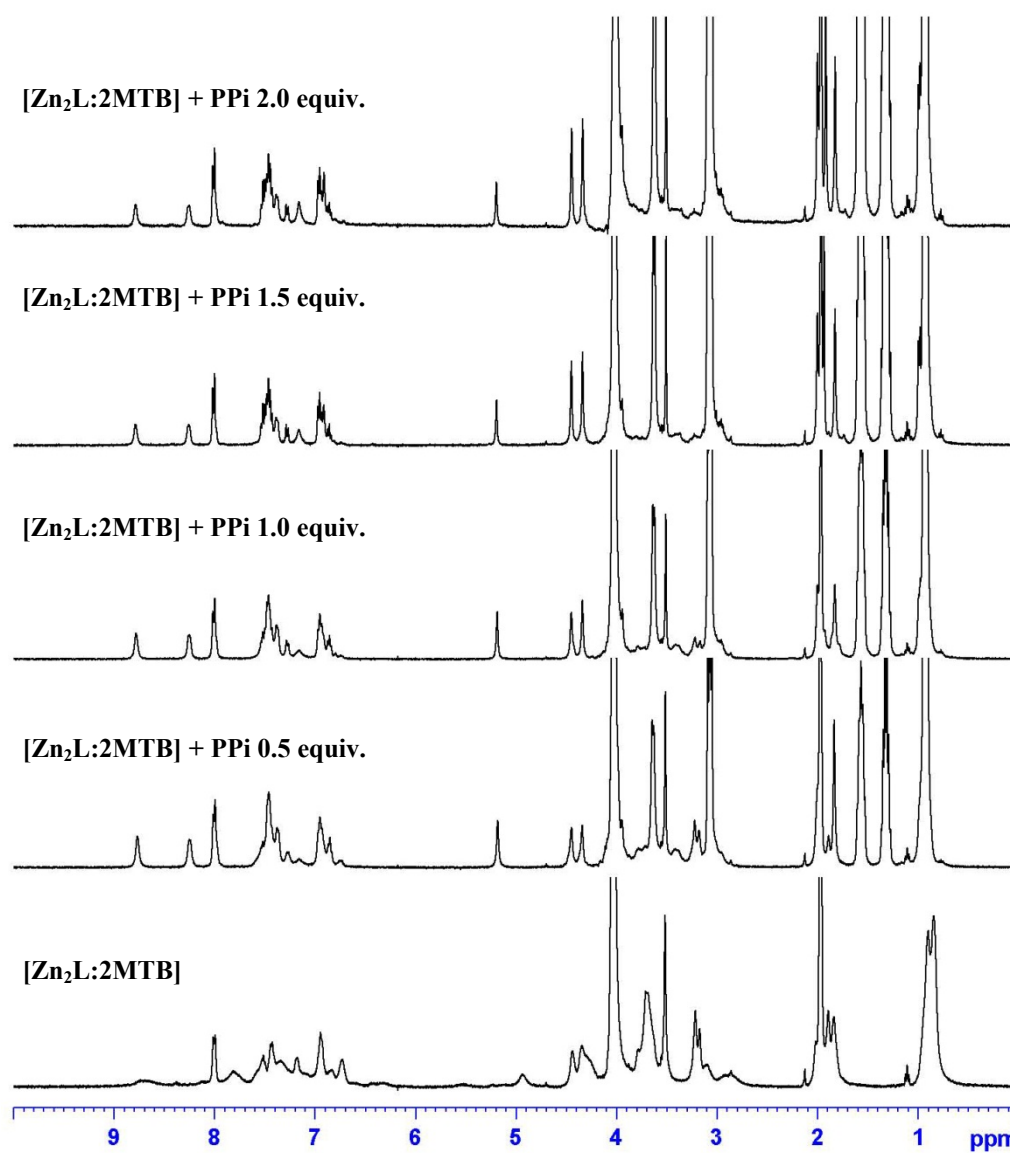


Figure S13. ^1H NMR spectra of 1:2 ratio of ensemble formation between $\text{Zn}_2\text{L}:\text{MTB}$ (5 mM) upon addition of various concentration of **PPI** (0.05 M) in 20% (v/v) $\text{D}_2\text{O}:\text{CD}_3\text{CN}$.

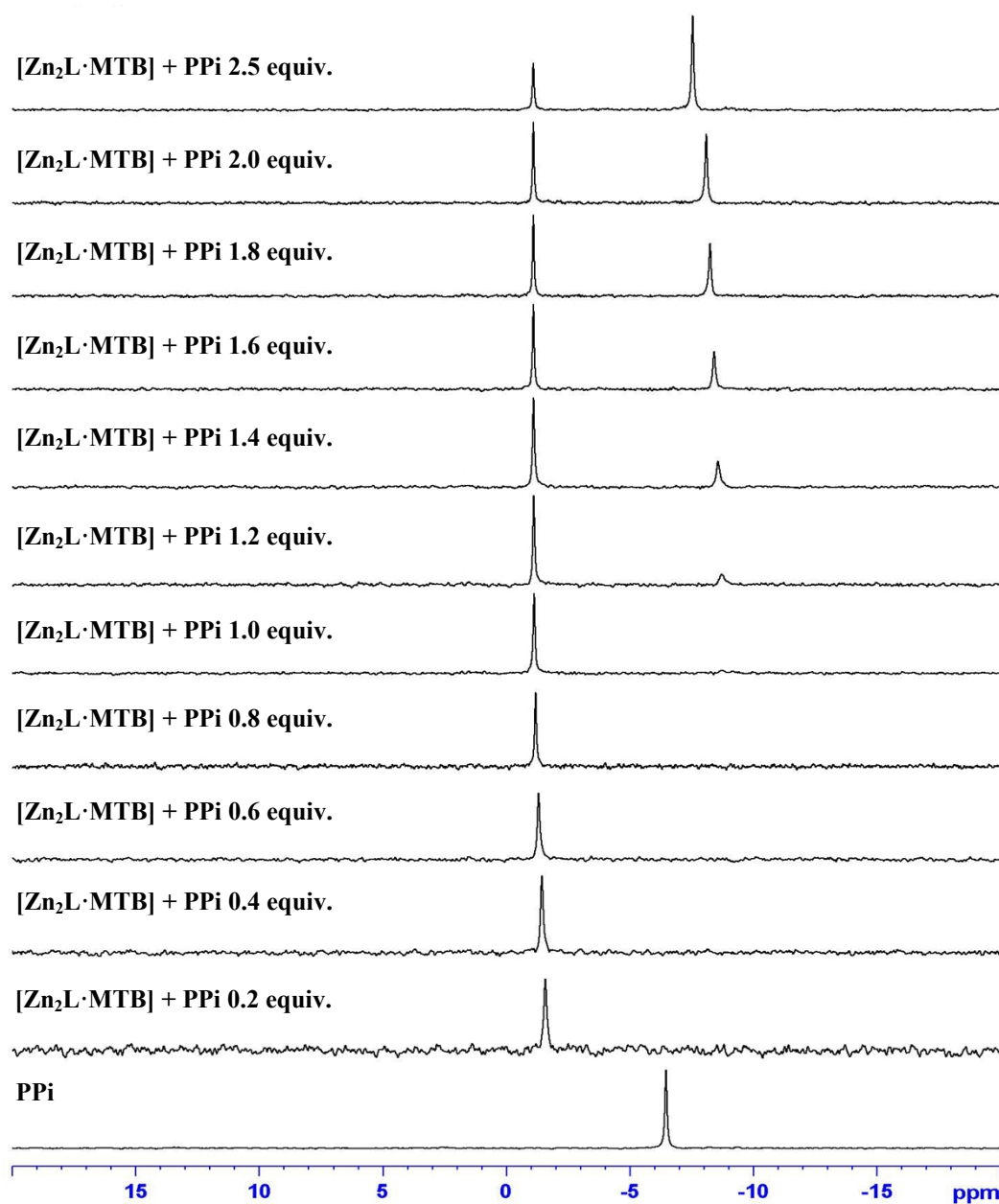


Fig S14. ^{31}P NMR spectra of $[\text{Zn}_2\text{L}\cdot\text{MTB}]$ (5 mM) upon addition of various concentrations of **PPI** (0.05 M) in 20% (v/v) $\text{D}_2\text{O}:\text{CD}_3\text{CN}$.

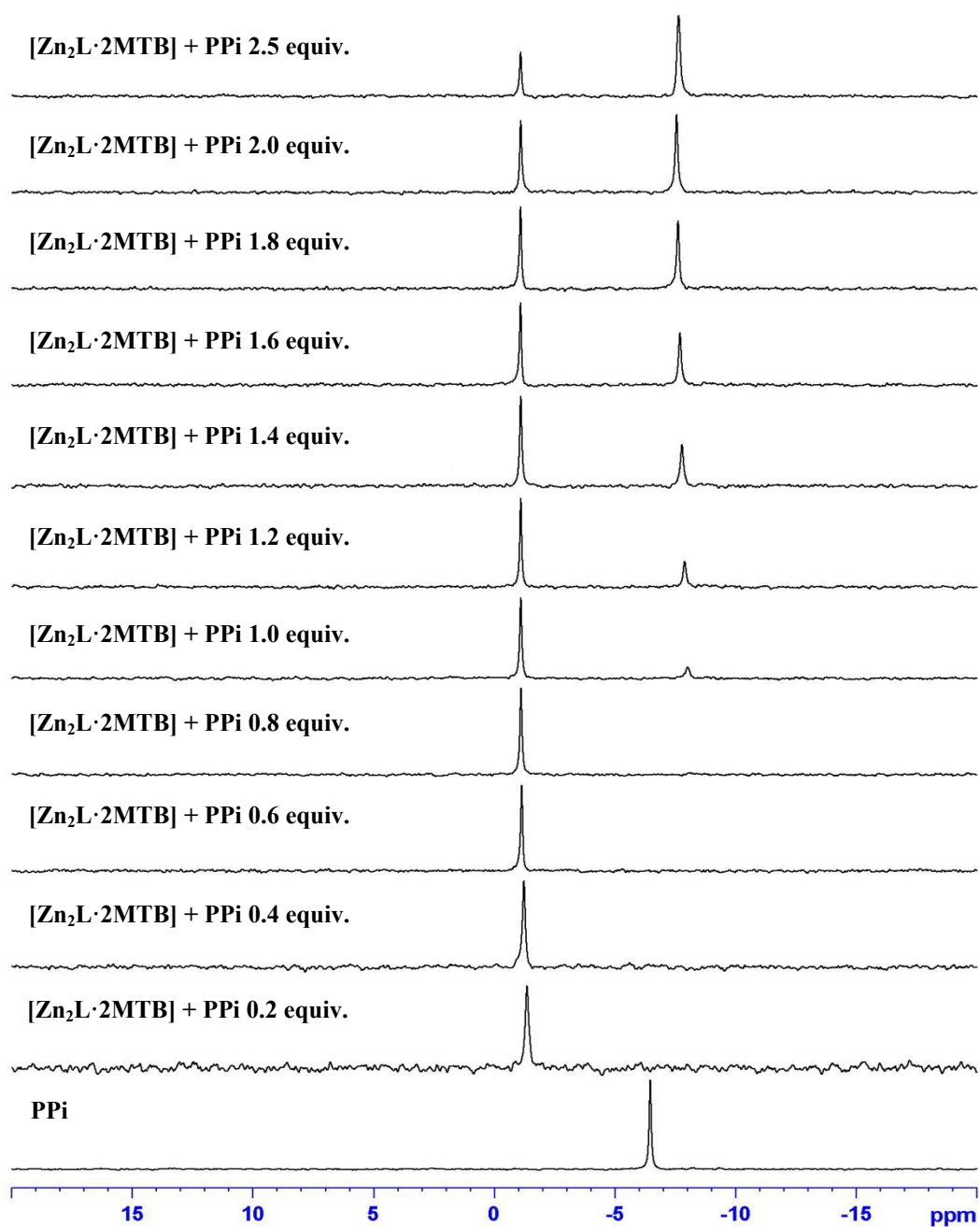


Fig S15. ^{31}P NMR spectra of $[\text{Zn}_2\text{L}\cdot 2\text{MTB}]$ (5 mM) upon addition of various concentrations of **PPI** (0.05 M) in 20% (v/v) $\text{D}_2\text{O}:\text{CD}_3\text{CN}$.

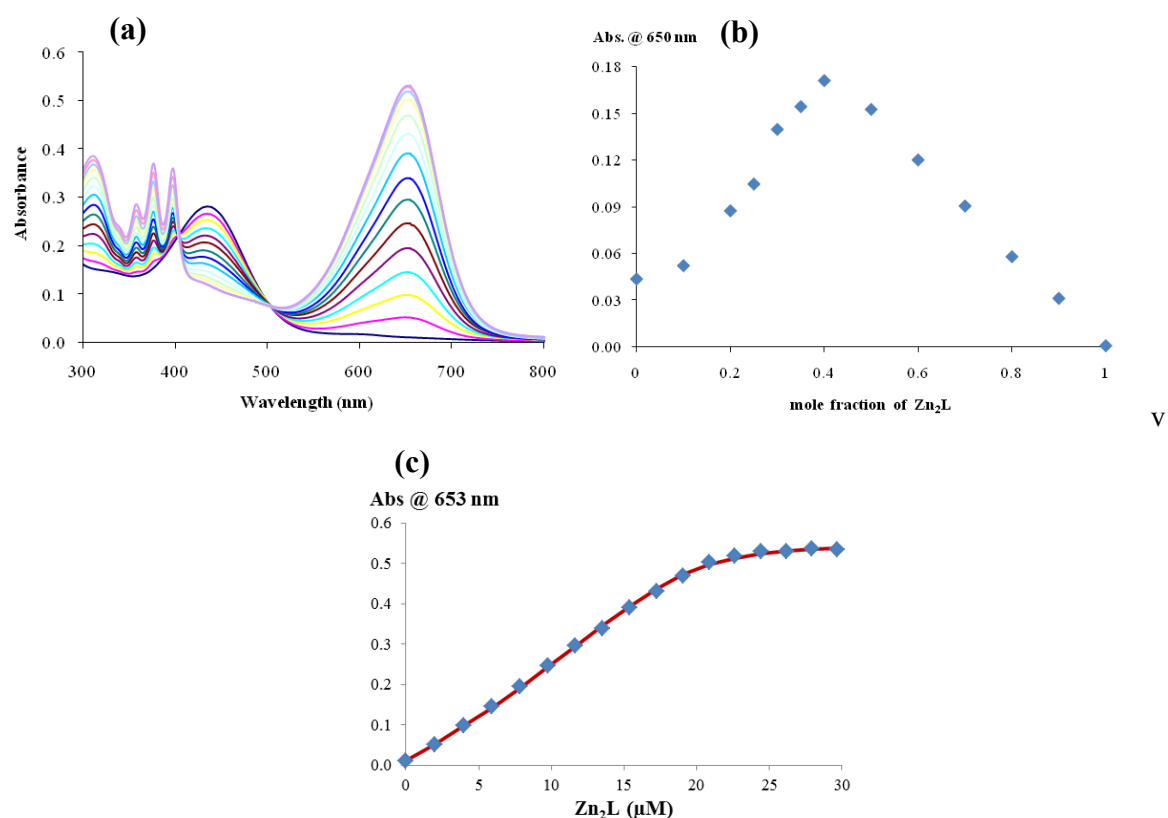


Figure S16. (a) UV/vis spectra obtained by addition of Zn_2L (400 μM) to a solution of indicator **PV** (20 μM) in HEPES buffered pH 7.4 in 20% (v/v) H_2O/CH_3CN solution, (b) Job's plot analysis of **PV**- Zn_2L ensemble, (c) A plot of absorption against concentration of Zn_2L titrated in **PV**. The red solid line is nonlinear least-squares fittings of the titration profiles using SPECFIT32 program.

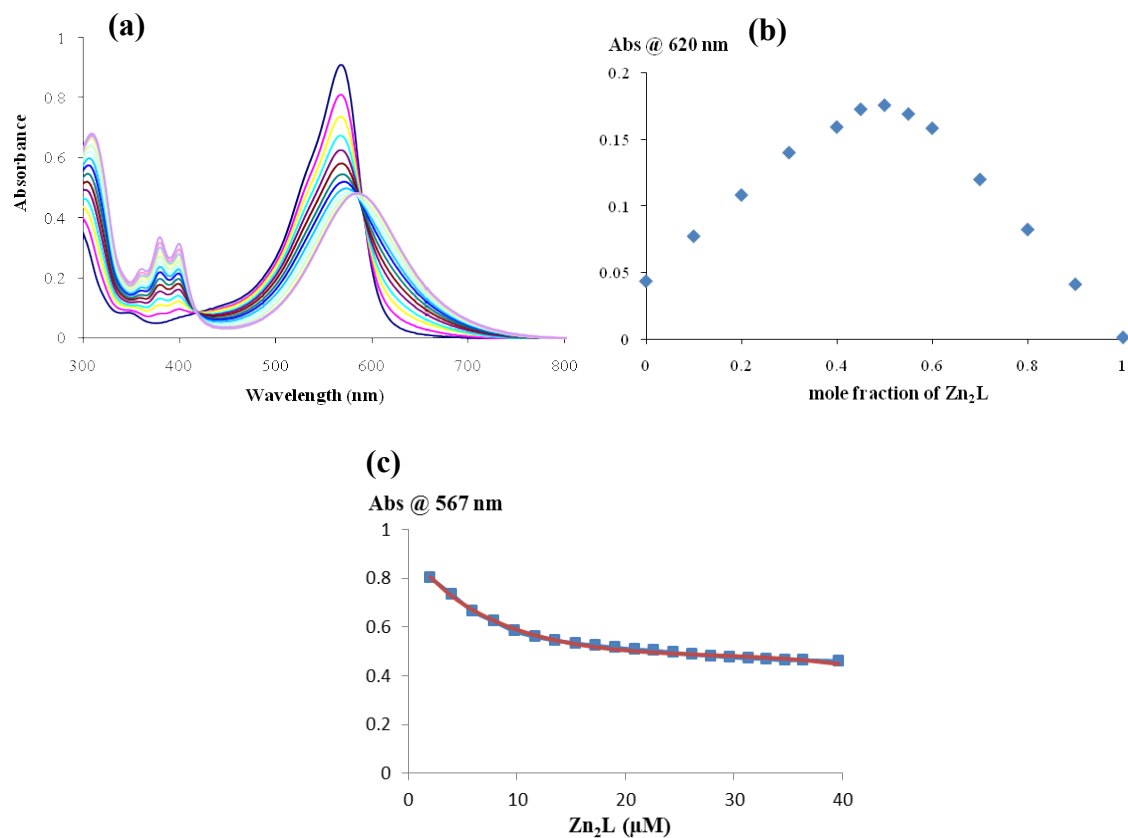


Figure S17. (a) UV/vis spectra obtained by addition of Zn_2L ($400\ \mu\text{M}$) to a solution of indicator **BPG** ($20\ \mu\text{M}$) in HEPES buffered pH 7.4 in 20% (v/v) $\text{H}_2\text{O}/\text{CH}_3\text{CN}$ solution, (b) Job's plot analysis of **BPG**- Zn_2L ensemble, (c) A plot of absorption against concentration of Zn_2L titrated in **BPG**. The red solid line is nonlinear least-squares fittings of the titration profiles using SPECFIT32 program.

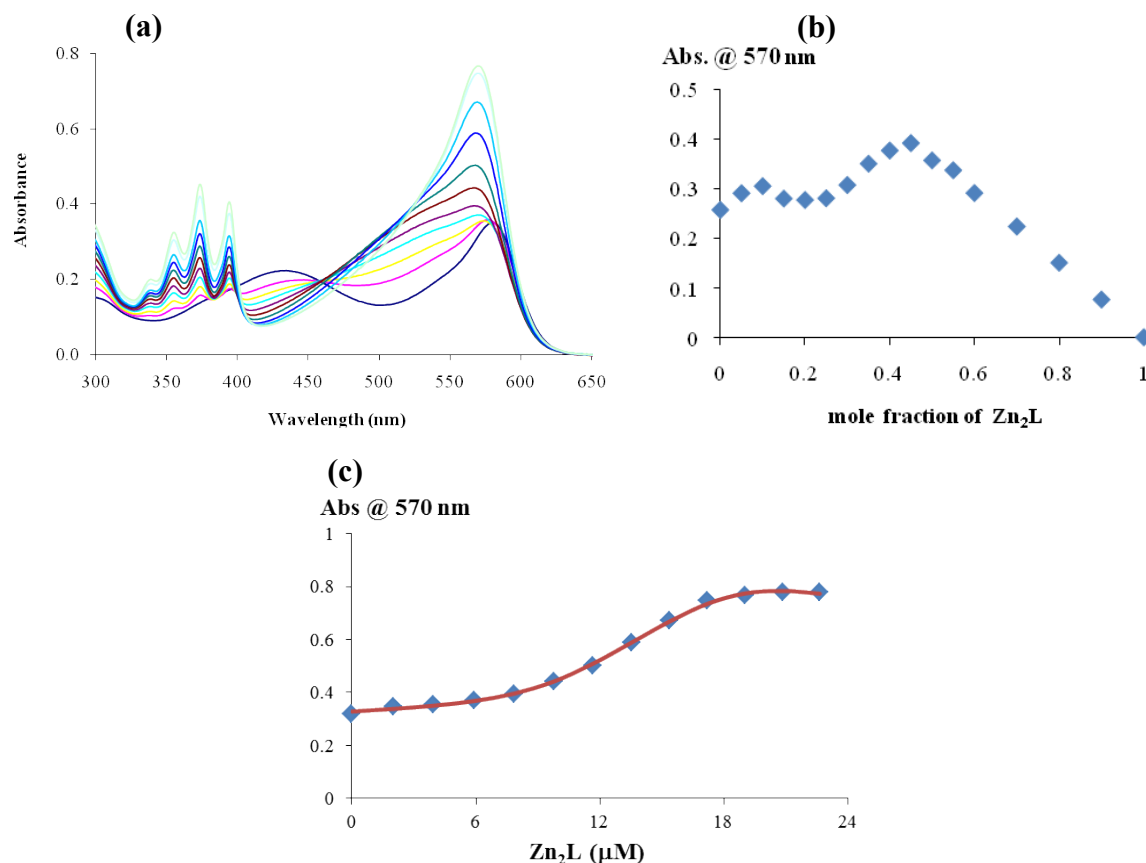


Figure S18. (a) UV/vis spectra obtained by addition of Zn_2L (400 μM) to a solution of indicator **XO** (20 μM) in HEPES buffered pH 7.4 in 80/20 (% v/v) $\text{CH}_3\text{CN}/\text{H}_2\text{O}$ solution, (b) Job's plot analysis of **XO**- Zn_2L ensemble, (c) A plot of absorption against concentration of Zn_2L titrated in **XO**. The red solid line is nonlinear least-squares fittings of the titration profiles using SPECFIT32 program.

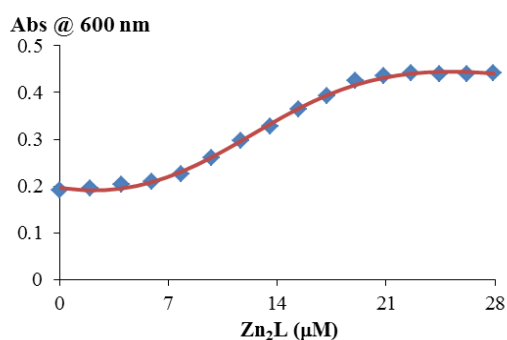


Figure S19. A plot of absorption against concentration of Zn_2L titrated in **MTB**. The red solid line is nonlinear least-squares fittings of the titration profiles using SPECFIT32 program.

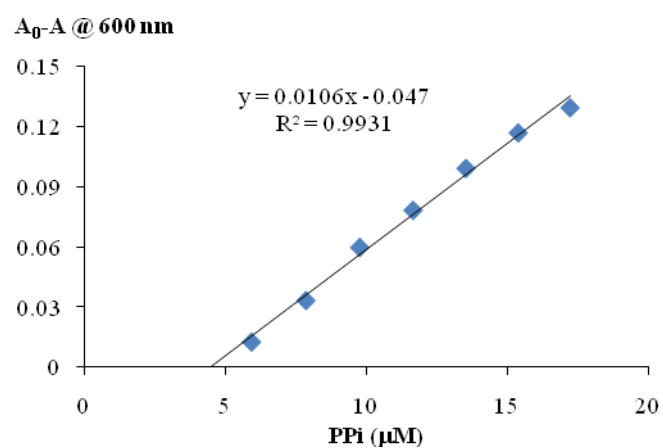


Figure S20. Calibration curve for detection of **PPI** using **MTB-Zn₂L** ensemble.